Photochemical & Photobiological Sciences

Accepted Manuscript

This is an *Accepted Manuscript*, which has been through the Royal Society of Chemistry peer review process and has been accepted for publication.

Accepted Manuscripts are published online shortly after acceptance, before technical editing, formatting and proof reading. Using this free service, authors can make their results available to the community, in citable form, before we publish the edited article. We will replace this *Accepted Manuscript* with the edited and formatted *Advance Article* as soon as it is available.

You can find more information about *Accepted Manuscripts* in the Information for Authors.

Please note that technical editing may introduce minor changes to the text and/or graphics, which may alter content. The journal's standard Terms & Conditions and the Ethical guidelines still apply. In no event shall the Royal Society of Chemistry be held responsible for any errors or omissions in this *Accepted Manuscript* or any consequences arising from the use of any information it contains.

ROYAL SOCIETY OF CHEMISTRY

www.rsc.org/pps

Journal Name

ARTICLE

Twisting in the Excited State of a N-Methylpyridinium Fluorescent Dye Modulated by Nano-Heterogeneous Micellar Systems

Received 00th January 20xx,
Accepted 00th January 20xx

DOI: 10.1039/x0xx00000x

www.rsc.org/

A. Cesaretti,[a,*] B. Carlotti,[a] P. L. Gentili,[a] R. Germani,[a] A. Spalletti,[a] F. Elisei[a]

A push-pull N-methylpyridinium fluorescent dye with a pyrenyl group as electron-donor portion was investigated within the nano-heterogeneous media provided by some micellar systems. The molecule was studied by stationary and time-resolved spectroscopic techniques in spherical micellar solutions and viscoelastic hydrogels, in order to cast light on the role played by twisting in its excited state deactivation. As proven by femtosecond fluorescence up-conversion and transient absorption experiments, the excited state dynamics of the molecule is ruled by charge transfer and twisting processes, which, from the locally excited (LE) state initially populated upon excitation, progressively lead to twisted (TICT) and planar (PICT) intramolecular charge transfer states. The inclusion within micellar aggregates was found to slow-down and/or limit the rotation of the molecule with respect to what had previously been observed in water, while its confinement within the hydrophobic domains of the gel matrixes determines the impossibility for any molecular torsion. The increasing viscosity of the medium, when passing from water to micellar systems, implies that the detected steady-state fluorescence comes from an excited state which is not fully relaxed, as is the case with the TICT state in micelles or the LE state in hydrogels, where the detected emission changes its usual orange colour into yellow.

Introduction

N-methylpyridinium-2-ethenyl-derivatives are widely studied compounds known to be extremely responsive to their immediate environment, as they show a net negative solvatochromic behaviour with increasing solvent polarity.[1-3] They can be used as fluorescent dyes to stain cellular compartments,[4-7] or else as non-linear optical materials for their high second order response due to the intramolecular charge transfer occurring in their excited state.[8-12] Moreover, they could also be exploited as drugs for their ability to bind the DNA-macromolecule.[13-16]

The great interest in their multipurpose applications pushed us to carefully look into the excited state properties of some molecules belonging to this family. In particular, in the past three years we have been investigating the spectral and kinetic behaviour of several of these *push-pull* compounds differing in the donor moiety from the parent 2-[4-(dimethylamino)styryl]-1-methylpyridinium iodide (o-DASPMI).[1,17-25] The nature of the electron-donor portion is indeed responsible for slightly different properties, which can be in turn modulated by guiding the choice toward the synthesis of new specific molecular systems.

In our laboratory, a great deal of attention has recently been devoted to a pyrenyl derivative of the DASPMI molecule, namely the 2-[(1-pyrenyl)-ethenyl]-1-methylpyridinium (Chart 1).[1,17,18,25] This flexible molecule could exist in fluid solution as an equilibrium mixture of four conformers that originate from the rotation around the quasi-single bonds between the aryl groups and the double bond. However, the computation of formation enthalpies (ΔH_f^0) revealed that the most stable and abundant (ca. 100% abundance) conformer at room temperature is the one shown in Chart 1.[1]

In the range of polarity covered by the investigated solvents, this molecule is completely dissolved without ion-pair formation and its photophysical properties are known to depend exclusively on its cationic part, which is highly sensitive to local environment.[1] Its absorption spectrum is subjected to a net negative solvatochromism and its emission is affected to a lesser degree by solvent polarity.[1]

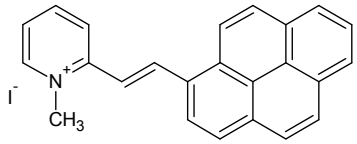

Chart 1. Molecular structure of *trans* (*E*) 2-(1-pyrenyl)-ethenyl-1-methylpyridinium iodide (***Pyr***).

The substantial negative solvatochromism shown by the molecule is due to a massive change in the dipole moment between the polar ground state and the moderately polar locally excited (LE) state.[1,25] The sharp difference in dipole moment determines a significant contribution to the second order term of the polarizability expansion, thus making the

[a] Department of Chemistry, Biology and Biotechnology and Centro di Eccellenza sui Materiali Innovativi Nanostrutturati (CEMIN), University of Perugia, via Elce di Sotto 8, 06123 Perugia, Italy. E-mail: alex.cesaretti14@gmail.com

investigated compound potentially interesting as NLO material.

However, the excited state deactivation patterns of the investigated compound have been interpreted taking into account the existence of other two emissive minima in S_1, formed from the moderately polar LE state by a back-charge transfer toward the pyrenyl portion mediated by twisting of the N-methylpyridinium ring.[25] These are intramolecular charge transfer (ICT) states characterized by high dipole moments and different geometries: a twisted ICT (TICT) state and a planar ICT (PICT) state, reached through progressive torsion around the quasi-single bond between the ethenic bridge and the methyl-pyridinium group of about 90° and 180°, respectively. This behaviour leads to a rotamer interconversion in S_1 toward the conformer which is absent in the ground state, thus contradicting the NEER (Non Equilibrated Excited Rotamers) principle.[25] The features of these ICT states also provide an explanation for the dependence of the spectral and kinetic behaviour showed by the molecule on the polarity and/or viscosity of the experienced solvent.[1,25]

Moreover, the pyrenyl derivative proved to be an efficient binder of the DNA macromolecule.[16] Linear dichroism measurements showed a mixed interaction mode, that is to say groove binding and intercalation, between the investigated N-methylpyridinium derivative and the DNA. A moderately high value of the binding constant was evaluated for it spectroscopically, which is especially interesting from a therapeutic point of view as far as its potential application as antitumor agent is concerned; a fact which is also corroborated by the anti-proliferative activity exhibited by some analogous compounds in preliminary *in vitro* tests.[26]

One major drawback in the use of this molecule for any practical application is its low water-solubility, which reduces its bioavailability. The aim of this paper is to find clever strategies to solubilize the investigated compound and to understand the modulation of its photobehaviour according to changes in its immediate environment. The pyrenyl derivative was therefore studied in micellar solutions of anionic surfactants (*i.e.* SDS and *p*OoBSK surfactants, cf. Chart 2), which might promote its solubilization,[23,27,28] and in surfactant hydrogels of intertwined wormlike micelles (made of zwitterionic *p*DoAO and cationic *Gemini* surfactants, cf. Chart 3),[24] which mimic the apolar and viscous domains of biological membranes: as the complexity of the investigated medium grows, deeper insights into the excited state dynamics of the molecule are gained and its peculiar response to local environmental changes is disclosed.

Results and discussion

Steady-State Absorption and Fluorescence. In aqueous solution and organic solvents, the investigated compound (***Pyr***) shows an absorption spectrum defined by two maxima (Figure S1).[1] The maximum at lower energy undergoes a negative solvatochromism, *i.e.* the band red-shifts by decreasing the solvent polarity, λ_{abs}= 420 nm in water (W) and 462 in dichloromethane (DCM): it can be attributed to the $S_0 \rightarrow S_1$ transition, occurring with a significant charge rearrangement. The maximum at higher energy is slightly affected by the polarity (λ_{abs}= 392 nm in W and 400 nm in DCM) and might be assigned to an upper π,π^* transition localized on the pyrene group, which is thus less sensitive to solvent properties.[1] As for its fluorescence spectra, the emission band shape and position remain almost insensitive to polarity, and the fluorescence quantum yield increases by just a 20% factor when going from W to the less polar and aprotic DCM (Table 1 and Figure S1). This fluorescence invariance has already been interpreted by invoking the charge transfer character of the emitting state, which, being highly polar as the ground state, gets equally stabilized in different solvents so that the emissive transition is almost insensitive to changes in polarity.[1]

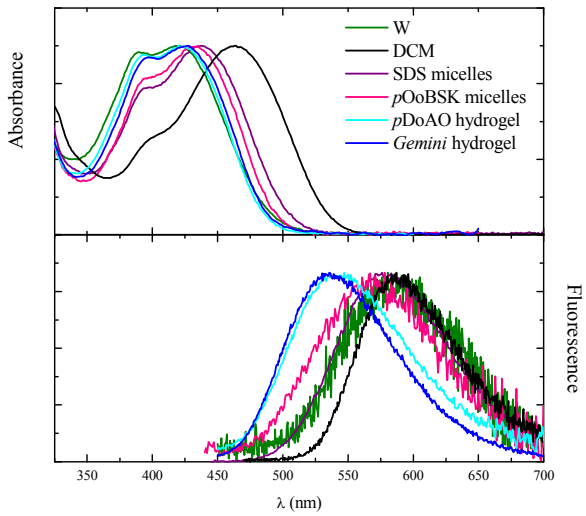

Figure 1. Normalized absorption and emission spectra of ***Pyr*** in W, DCM, SDS micelles, *p*OoBSK micelles, *p*DoAO hydrogel and *Gemini* hydrogel.

When ***Pyr*** is dissolved in micellar aqueous solution and hydrogels, significant spectral alterations are observed (Figure 1). Both micelles enhance the solubility of the molecule, supposedly as a result of an efficient inclusion within the surfactant aggregates. From a spectral point of view, this inclusion is responsible for a pronounced bathochromic shift of the long-wavelength absorption maximum (up to 438 nm in SDS micelles) and a little hypsochromic shift of the emission band with respect to pure water; on the other hand, the absorption properties within both surfactant hydrogels are affected to a lesser extent, whereas the emission spectrum results blue-shifted by nearly 50 nm when compared to the fluorescence observed in aqueous solution (Figure 1). The alterations induced by the hydrogels are larger in the more viscous *Gemini* hydrogel, where the *Stokes shift* declines from the value of 6740 cm^{-1} in water to 4730 cm^{-1} within the gel matrix. A marked reduction of the *Stokes shift* is typical of molecules confined in a rigid nano-environment like the one offered by the intertwined elongated micelles, as confirmed by

the increment of the fluorescence quantum yields of more than two times (Table 1).

Table 1. Spectral and fluorescence properties of ***Pyr*** in W, DCM, SDS micelles, *p*OoBSK micelles, *p*DoAO hydrogel and *Gemini* hydrogel.

Medium	λ_{abs}/nm	λ_{em}/nm	$\Delta\nu$ /cm^{-1}	ϕ_F	τ_F /ps	k_F /s^{-1}
W[a]	390, 420	586	6740	0.028	300	$9.3\cdot10^7$
DCM[a]	400, 463	588	4590	0.033	-	-
SDS micelles	397, 438	578	5530	0.079	550	$1.4\cdot10^8$
*p*OoBSK micelles	395, 432	568	5540	0.050	430	$1.2\cdot10^8$
*p*DoAO hydrogel	393, 422	540	5180	0.068	520	$1.3\cdot10^8$
Gemini hydrogel	396, 427	535	4730	0.066	720	$9.2\cdot10^7$

[a]Data retrieved from ref. 1.

In order to rationalize the changes in the spectral properties observed in the presence of micelles in terms of an effective interaction with the supramolecular assembly, the compound was investigated by adding growing amounts of anionic surfactants to its initial aqueous solutions.

The peculiar evolution of the absorption and fluorescence spectra of ***Pyr*** during the titration is shown in Figure S2. A double trend (before and after the c.m.c. values) is observed in the presence of both surfactants, although some differences can be detected between the two of them. The determination of any quantitative parameter to describe the interaction (such as binding constant or stoichiometry) was however prevented by the detection of scattered light at long wavelengths, particularly visible as a tail in the absorption band when titrating with *p*OoBSK (cf. Figure S2, bottom left panel), that may indicate the formation of poorly soluble ion pairs.

As far as SDS surfactant is concerned, the interaction between the cationic dye and the anionic surfactant monomers, active at low concentration of surfactant, causes a drop in the absorbance of the long-wavelength absorption band while the other band, associated with the π,π* transition on the aromatic pyrene group, is less affected (Figure S2 upper left panel, red spectra), in accordance with an electrostatic interaction with the surfactant mainly involving the cationic pyridinium ring. Simultaneously, the emission intensity decreases, with the appearance of a new maximum at longer wavelength (~ 710 nm, Figure S2 upper right panel, red spectra). The electrostatic interaction between ***Pyr*** and the surfactant could be responsible for the formation of ***Pyr*** excimers when two or more pyrenes are forced together in a sub-micellar cluster. Pyrene is indeed known to form excimers at high concentration in solution; in like manner, the presence of charged detergent molecules could induce high local concentrations of ***Pyr*** around the anionic surfactants leading to excimer emission at longer wavelength with respect to that of monomeric ***Pyr***. Conversely, the interaction of ***Pyr*** with the *p*OoBSK surfactant molecules seems to be less selective for the methyl-pyridinium unit: a plausible further interaction between the surfactant aromatic ring and the equally aromatic pyrene group has to be invoked, thus affecting the whole absorption spectrum (Figure S2 lower left panel, red spectra). The fluorescence emission is red-shifted and reduced to a minor degree (λ_{max} = 630 nm, Figure S2 lower right panel, red spectra), supposedly because of a competition between the π-π pyrene-pyrene interaction, which would lead to the excimer emission around 700 nm, and the π-π pyrene-surfactant interaction.

When the c.m.c. is reached, the formation of the micelles is responsible for the typical spectral changes associated with an efficient inclusion of the compound within the scarcely polar and highly confining environment granted by the micellar aggregate (Figure S2, black spectra):[29,30] namely the enhancement of the absorption and emission intensities and the fluorescence blue-shift.

Fluorescence Kinetic Investigation and MEM Analysis. The kinetic behaviour exhibited by the fluorescent dye was investigated by means of the *time correlated single photon counting* (TC-SPC) technique. The fitting of the kinetic traces by mono-exponential functions gives back the mean lifetime values reported in Table 1. The fluorescent excited state lifetime slightly increases when passing from W to the diverse organized media. These little changes in the lifetimes and in the ϕ_F determine fluorescent constants of about $1\cdot10^8$ s^{-1}, weakly dependent on the medium (cf. Table 1); they reveal that the main emission transition is always allowed.

In fact, the fitting obtained by the single exponential analysis of the data in the nano-heterogeneous micellar systems (especially in hydrogels) were described by χ^2 parameters which move away from unity, and the calculated lifetimes were only taken as average values to compare with the lifetime in water. The decay kinetics were thus analysed by the Maximum Entropy Method (MEM), in order to get a deeper insight into the nano-heterogeneity of the molecular surrounding.

The results of the MEM analysis are indeed very impressive and disclose utterly different scenarios, as it is shown in Figure 2. In pure aqueous solution, the emission gives rise to a sharp peak (olive trace) around 350 ps proving the homogeneous character of the solvent. In the two types of micelles, the detected emission (pink and purple traces) are characterized by broadened dispersions around average times of nearly 400 and 600 ps in *p*OoBSK and SDS micelles, respectively. These broadened time dispersions demonstrate that anionic micelles provide ***Pyr*** with a rather heterogeneous environment. The spatial disposition of the surfactants in three-dimensional networks causes ***Pyr*** to experience varied immediate environments in the same sample, in that it can be more exposed to the hydrophobic domains formed by the surfactant assemblies or to the more polar hydrophilic heads.

In both hydrogels, the distributions of lifetimes (cyan and blue traces) become much broader, thus revealing a greater heterogeneity for these nano-scaled organized media. Their maxima match the average time found by the mono-exponential fitting (cf. Table 1), but a tail around 100 ps also makes a contribution to the time dispersion. This asymmetric broadening may account for the emission coming from upper states of the excited molecule, which might be worth to be examined by means of ultrafast spectroscopic techniques.

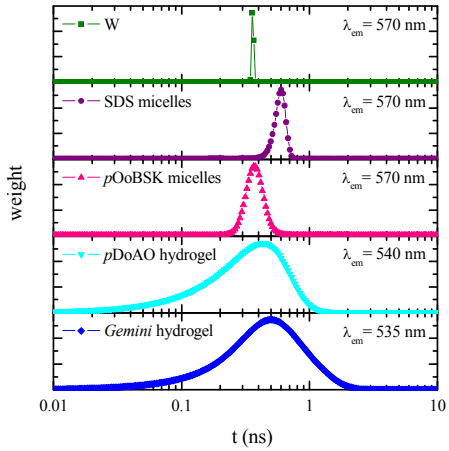

Figure 2. Results of the analysis carried out by the Maximum Entropy Method on the kinetics acquired by the time correlated single photon counting technique of ***Pyr*** (λ_{exc}= 461 nm) in W (olive trace), SDS micelles (purple trace), *p*OoBSK micelles (pink trace), *p*DoAO hydrogel (cyan trace) and *Gemini* hydrogel (blue trace).

Femtosecond Fluorescence Up-Conversion. The fluorescence up-conversion spectral evolution of ***Pyr*** in the two micellar media is described by a dynamical *Stokes shift* which eventually leads to the position of the stationary fluorescence (Figure 3). Target Analysis revealed three components for the deactivation of ***Pyr*** in both types of micelles, but the different spectral shapes of the transients guided their assignment to distinct emissive species in the two environments (Table 2). These assignments are corroborated by the Time Resolved Area Normalized Emission Spectra (TRANES) analysis performed on the up-conversion data and shown in Figure S3 and S4. When the TRANES evolution is characterized by the appearance of *n* isoemissive points, the existence of *n+1* different emissive minima describing the time resolved fluorescence of a molecule can be deduced. The search for the isoemissive points must be conducted in those particular delay time intervals where there are only two species mainly contributing to the fluorescence (cf. concentration profiles in Figure S3 and S4.).

In the case of ***Pyr*** in SDS micelles (Figure 3, left graph), the TRANES evolution, shown in Figure S3, features *n* = 2 isoemissive points, which implies that each of the 3 transients accounts for an emissive species involved in the deactivation of ***Pyr***. The first transient is defined by a time constant of 2.4 ps and features a bell-shaped band centred at about 545 nm. It can be assigned to a low polar LE state, populated upon excitation, decaying to a second minimum along with solvation (first isoemissive point). A decaying component of 2.4 ps can indeed be detected at the LE emission wavelength (508 nm, cf. Figure S5), whereas a rising component characterized by the same time constant is observed at longer wavelengths (610 nm), implying the population of a second minimum. The intermediate component, with a lifetime of 91 ps, shows instead a broad spectrum, red-shifted with respect to the LE emission, and likely due to the emission from a stabilized ICT minimum. This latter then gives a longer-living emitting species (second isoemissive point), originating a fluorescence band centred at 585 nm, which is apparently narrower than that of the intermediate transient. The reduction of the band width during the transition between the last two transients may be the sign of a plausible planarization of the ICT state, which passes from a twisted geometry (TICT) to a planar one (PICT). More precisely, as previously suggested by vibronic computations based on density functional potential energy surfaces and supported by data acquired in water,[25] the two ICT states are likely reached by progressive torsion around the quasi-single bond between the methyl-pyridinium and the double bond.

The spectral shapes of the three transients calculated in nano-heterogeneous micellar solution invite comparison with what was found in homogenous aqueous solution (Table 2). Close similarity exists for the LE and PICT states because of the planar geometry taken on by the molecule in the two minima, whereas the difference in the spectral shape of the TICT state may arise from its twisted geometry. As a matter of fact, the position of the TICT state, slightly blue-shifted when compared with the same transient in water (570 nm vs 585 nm),[25] may account for the viscosity and heterogeneity of the micellar medium, which is indeed expected to hinder the rotation around the quasi-single bond. This may give rise to a variety of conformations, featuring a progressive degree of twisting, contributing to the fluorescence, and only eventually leading to the fully relaxed, *i.e.* completely twisted, ICT state.

Notwithstanding the similar lifetimes found for ***Pyr*** in *p*OoBSK solution, the assignment of the three components in this medium is not as trivial as it might seem, but the spectral shapes (Figure 3C, right graph) and TRANES evolution (Figure S4) are instrumental in helping to uncover the nature of the three transients. The first component of 2.8 ps is centred at 530 nm, whereas the second component of 81 ps peaks at 545 nm. Between these two transient no isoemissive point can be spotted in the TRANES evolution, which is instead characterized by a red-shift of the time resolved fluorescence. This means that the evolution from the first transient to the other is a pure solvation step and not a transition between two distinct states. In fact, as it emerges from the continuous shift in the TRANES, solvation does provide the molecule with a continuum of states. The two transients can be thus assigned to the solvent relaxation around the excited state and the relaxed LE minimum, respectively. The LE state then evolves to the third transient, defining a clear isoemissive point (Figure

S4) and therefore allowing its assignment to a second minimum. This emissive state is labelled as a twisted ICT state, in that it outlines, like the TICT minimum in SDS, a broad spectrum centred at 575 nm, although it decays directly to the ground state with a lifetime of 380 ps. In the presence of *p*OoBSK micelles, a rise-decay dynamics of tens of picoseconds is peculiar to the fluorescence up-conversion kinetics of ***Pyr*** (Figure S5), which indeed undergoes a slowed-down charge separation in the excited state, supposedly because of a specific interaction between the surfactant monomers and the dye, which limits the charge migration processes and the torsions occurring with them. This implies, on the one hand, the possibility to tell apart the solvent re-equilibration ($\tau_{Solv.}$ = 2.8 ps) from the LE deactivation (τ_{LE} = 81 ps, $k_{LE\rightarrow TICT} = 1.2\cdot10^{10}$ s^{-1}), which becomes much slower than it is in water (τ_{LE} = 1.0 ps, $k_{LE\rightarrow TICT} = 1.0\cdot10^{12}$ s^{-1}) or even in SDS micellar solutions (τ_{LE} = 2.4 ps, $k_{LE\rightarrow TICT} = 4.2\cdot10^{11}$ s^{-1}), and, on the other hand, the inability for ***Pyr*** to populate the final PICT state.

Moreover, by critically looking at the steady-state fluorescence spectra (cf. Figure 1, bottom panel), an atypical broadening toward higher energies can be noticed in the case of ***Pyr*** in *p*OoBSK micelles. The emission might originate from the TICT state, which is the last excited-state minimum reached during the deactivation in this medium and might exist, because of the nano-heterogeneous environment provided by the micelles, in a vast number of conformations obtained by progressive torsion of the molecule. The conformational disorder of the TICT state can therefore be responsible for the spectral broadening peculiar to the steady-state fluorescence within *p*OoBSK micelles and can also contribute to the larger temporal dispersion revealed by the MEM analysis in this medium with respect to SDS micelles, where the detected fluorescence comes, instead, from the PICT state (cf. Figure 2).

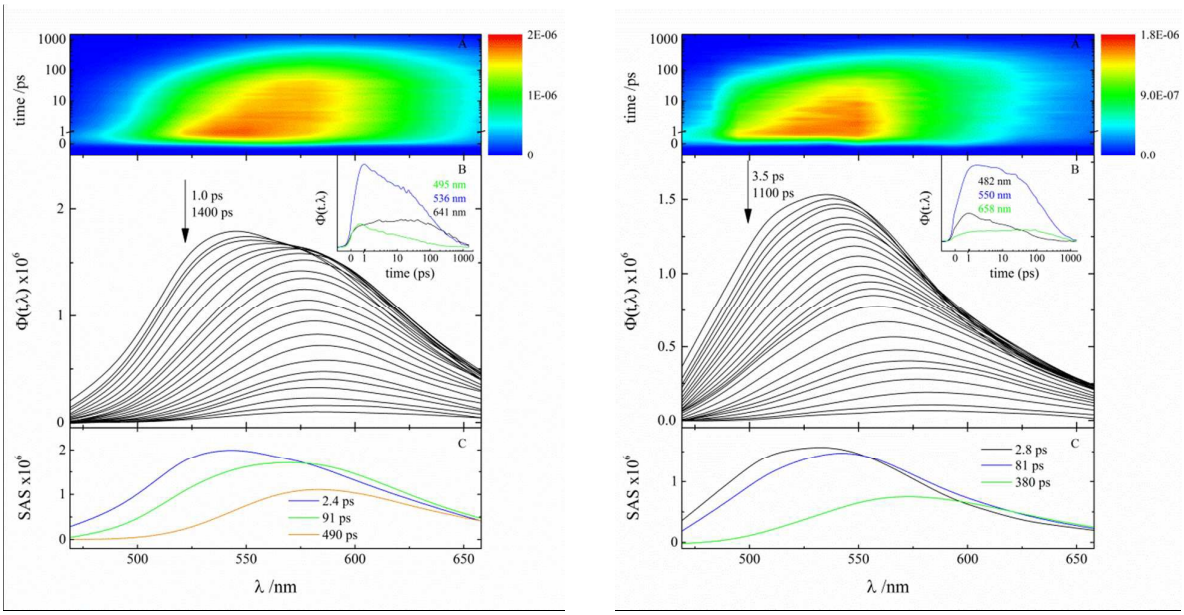

Figure 3. Fluorescence up-conversion spectroscopy of ***Pyr*** in SDS (left graph) and *p*OoBSK (right graph) micelles (λ_{exc} = 400 nm): (A) contour plot of the experimental data, (B) time-resolved emission spectra recorded at increasing delays after the laser pulse (inset: decay kinetics at meaningful wavelengths, with a linear scale for the first picoseconds and a *log* scale for longer times), and (C) Species Associated Spectra (SAS) calculated by Target Analysis.

Table 2. Excited state spectral and kinetic properties of ***Pyr*** in W, SDS micelles and *p*OoBSK micelles obtained by femtosecond fluorescence up-conversion spectroscopy (λ_{exc} = 400 nm).[a]

Medium	*λ /nm*	*τ /ps*	***Assignment***
W[b]	**550**	**1.0**	**Solv./^{1}LE***
	585	**40**	**^{1}TICT***
	585	**270**	**^{1}PICT***
SDS micelles	**545**	**2.4**	**Solv./^{1}LE***
	570	**91**	**^{1}TICT***
	585	**490**	**^{1}PICT***
*p*OoBSK micelles	530	2.8	Solv.
	545	**81**	**^{1}LE***
	575	**380**	**^{1}TICT***

[a]Spectral properties refer to the Species Associated Spectra (SAS) calculated by Target Analysis.
[b]Data retrieved from ref.25.

Table 3. Excited state spectral and kinetic properties of ***Pyr*** in W, DCM, SDS micelles, *p*OoBSK micelles, *p*DoAO hydrogel and *Gemini* hydrogel obtained by femtosecond transient absorption spectroscopy (λ_{exc} = 400 nm).[a]

Medium	*λ /nm*	*τ /ps*	***Assignment***
W[b]	650(+)	0.1	Solv.
	550(+)	**1.1**	**Solv./^{1}LE***
	540(+), 645(–)	**20**	**^{1}TICT***
	535(+), 630(–)	**275**	**^{1}PICT***
DCM[b]	**590(+)**	**1.3**	**Solv./ ^{1}LE***
	550(+), 640(–)	**34**	**^{1}TICT***
	545(+), 630(–)	**424**	**^{1}PICT***
SDS micelles	520(–), 625(+)	0.49	Solv.
	590(+)	**4.7**	**Solv./^{1}LE***
	560(+)	**61**	**^{1}TICT***
	545(+), 630(–)	**470**	**^{1}PICT***
*p*OoBSK micelles	510(–), 635(+)	0.29	Solv.
	525(–), 625(+)	6.3	Solv.
	600(+)	**80**	**^{1}LE***
	555(+), 650(–)	**430**	**^{1}TICT***
*p*DoAO hydrogel	515(–), 635(+)	5.5	Solv.
	525(–), 615(+)	100	Solv.
	580(+)	**440**	**^{1}LE***
Gemini hydrogel	515(–), 635(+)	2.7	Solv.
	525(–), 625(+)	81	Solv.
	590(+)	**680**	**^{1}LE***

[a]Spectral properties refer to the Species Associated Spectra (SAS) calculated by Target Analysis. The symbols (+) and (–) stand for positive and negative signals, respectively.

[b]Data retrieved from ref. 1. The assignments were revised according to the new mechanistic interpretation of ref. 25.

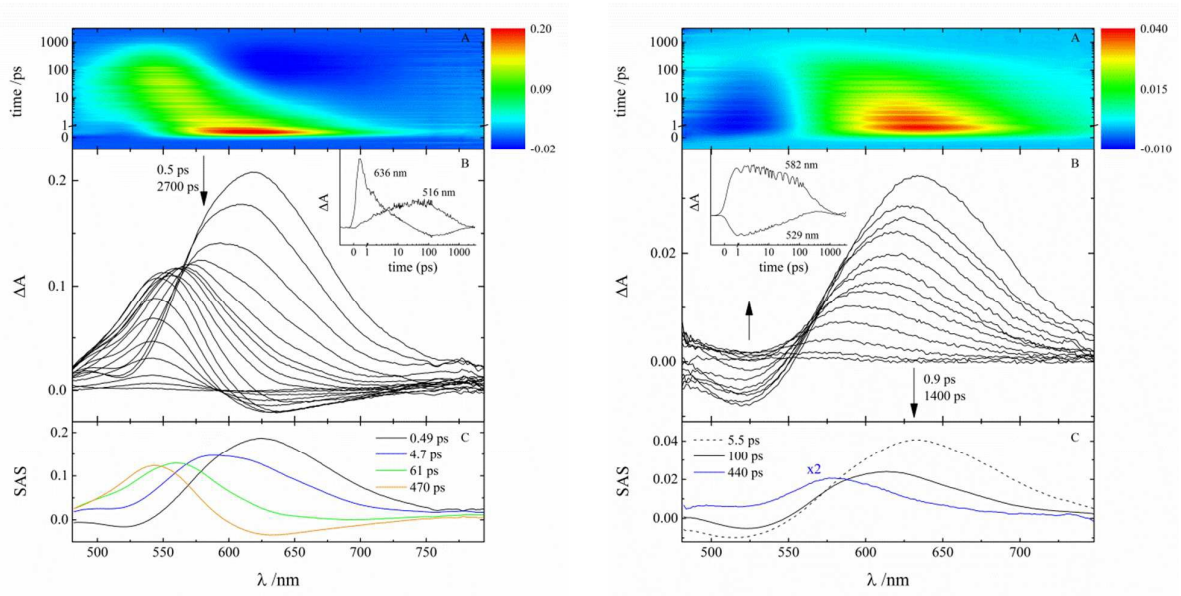

Figure 4. Pump-probe absorption spectroscopy of ***Pyr*** in SDS micelles (left graph) and *p*DoAO hydrogel (right graph) (λ_{exc} = 400 nm): (A) contour plot of the experimental data, (B) time-resolved absorption spectra recorded at increasing delays after the laser pulse (inset: decay kinetics at meaningful wavelengths, with a linear scale for the first picoseconds and a *log* scale for longer times), and (C) Species Associated Spectra (SAS) calculated by Target Analysis.

Femtosecond Transient Absorption. The excited state dynamics of the investigated compound in all of the considered organized media was also studied by means of femtosecond transient absorption experiments. The results of the Target Analysis are shown in panel C of Figures 4 and Figures S6-S7, and listed in Table 3, together with data

referring to the same molecule in the polar aqueous solution (W) and in the less polar DCM.

As previously observed in non-surfactant solutions,[1] the time resolved spectra of the compound are dominated by positive signals of excited state absorption (ESA), which shift over time toward the blue side of the spectrum. The shifts are due to the stabilization of the excited state of the molecule: the larger the shift, the more the excited state gets stabilized. However, corroborating what was inferred from the fluorescence up-conversion measurements, the behaviour shown by ***Pyr*** is quite different in the two types of anionic micelles (Figure 4, left graph and Figure S6): in the case of SDS micelles a positive signal of transient absorption arises around 625 nm; it then undergoes a major *blue-shift* up to 540 nm, while a little negative signal of stimulated emission appears at longer wavelengths. Conversely, in the presence of *p*OoBSK micelles ***Pyr*** still gives a signal of transient absorption centred at 625 nm, but also a negative band of stimulated emission at about 525 nm. The former band moves towards higher energies while decaying, overshadowing the negative signal, but in this case no formation of stimulated emission is clearly observed in the red part of the spectrum at longer delays. As for the two surfactant hydrogels, the spectral evolution is similar to that recorded in *p*OoBSK solutions, but reduced shifts are peculiar to the molecule within the gel matrixes, especially in the case of the *Gemini* gel (cf. Figures 4, S6 and S7).

As it is already clear from the observation of the spectral evolution, the two micellar media have a different influence on the excited state dynamics of ***Pyr***. As far as SDS micelles are concerned, four exponentials define the decay kinetics of ***Pyr***: a sub-picosecond short component ($\tau_{Solv.}$ = 0.49 ps) assigned to inertial solvent equilibration and missed in the analogous up-conversion experiment due to the lower temporal resolution of this latter technique, a short component mixed with diffusive solvation and attributed to the LE state (τ_{LE} = 4.7 ps), and two longer-living components associated with the TICT and PICT states (τ_{TICT} = 61 ps and τ_{PICT} = 470 ps, respectively). These assignments are again supported by spectral comparison with the transients observed in non-surfactant solutions.[1] The spectral matching among the SAS is fairly good, especially when they are compared with those obtained in the poorly polar DCM (Table 3). The only apparent discordance regards the TICT state, whose transient absorption is slightly red-shifted in SDS solution, revealing the incomplete relaxation of the twisted state within the micelles, validating its blue-shifted emission previously observed through the fluorescence up-conversion experiment. This can be reasonably explained considering the different degrees of rotation (and thus of stabilization) reached by molecules in the TICT state within the nano-heterogeneous environment typical of the micellar solution. However, a good lifetime correspondence with the organic solvent is only observed for the PICT state, while both the LE and TICT transients, which require torsions for their deactivation, are described by longer times. All of these findings support the hypothesis of an efficient inclusion of the compound within the surfactant aggregates, where the molecules experience a less polar and more viscous microenvironment than the polar and non-viscous bulk aqueous solution.

In the case of *p*OoBSK micelles, the shift over time of the main femtosecond transient absorption band is smaller than that observed in both solution and SDS micelles, which means a reduced stabilization reached in the excited state. The Target Analysis of the time-resolved absorption spectra revealed four components. Apart from a typical ultrafast solvent equilibration occurring in 0.29 ps and another short relaxation ($\tau_{Solv.}$ = 6.3 ps, although slowed-down for water molecules in the Stern layer of a micelle with respect to free water),[31-33] the spectral shapes of the other two transients are very straightforward. On the one hand, the intermediate component (λ_{max} = 600 nm and τ = 80 ps) features a SAS which is quite similar to that of the LE transient observed in W, DCM and SDS solutions and thus assigned to the same state.[1] In fact, in non-surfactant solution the LE state quickly evolves toward a TICT state during the solvation stage, while in the more viscous SDS solution the back-charge transfer mediated by twisting of the N-methylpyridinium gets slower. In the presence of *p*OoBSK micelles, where a specific π-π interaction adds its contribution to the micro-viscosity of the micellar medium, the TICT formation is considerably slowed down and the solvent equilibration and LE deactivation get well-separated in time. On the other hand, the spectrum associated with the longer-living component (λ_{max} = 555 nm and τ = 430 ps) resembles that of the polar TICT state observed in SDS solution and thus assigned to it. In keeping with the up-conversion results, no evidence of the formation of a further PICT state arises from the ESA experiment either.

The femtosecond transient absorption experiments performed in hydrogels revealed a spectral evolution similar to that observed in the presence of *p*OoBSK micelles. A comparison with the micellar medium is indeed needed, as the phenyl ring of the anionic surfactant, which is a common feature with the two gel-forming surfactants, proved to significantly influence the excite state dynamics of ***Pyr***.

Differently from other analogous compounds which were found to distribute between the aqueous pools and hydrophobic domains of the gel,[24] the excited state dynamics of ***Pyr*** does not offer any evidence of the presence of some molecules in water, since the Species Associated Spectra and their associated lifetimes do not match the time constants and spectral shapes of the transients observed in water (Figure 8 and Table 3). In fact, the pyrenyl substituent provides the molecule with a marked hydrophobic character and a preferential portioning in the gel phase can be envisaged taking place. However, the little bathochromic shift of the steady-state absorption maxima, which is smaller than the shift observed in *p*OoBSK micelles (cf. Table 1), suggests that in the presence of the anionic micelles, driven by the electrostatic attraction with the surfactant heads, ***Pyr*** is able to go deep inside the scarcely polar micellar aggregate, whereas in zwitterionic or dicationic hydrogels the same molecule does not penetrate within the non-polar micelles but it probably gets stuck between the charged walls of intertwined micelles, experiencing a rather polar environment.

Based on the knowledge acquired from the analysis performed in the presence of anionic micelles, the deactivation can be interpreted as follows. The fast and intermediate components (5.5 ps and 100 ps in *p*DoAO Gel and 2.7 and 81 ps in *Gemini* Gel), whose SAS follow those of the fastest transients found in micelles, are assigned to solvation processes which may also bear a vibrational cooling contribution. Their lifetimes, much longer than typical solvation found in the other media, are due to the non-diffusing character of the gel matrixes, where bound water molecules are known to exhibit dramatically slow solvation dynamics.[31,34-36] The longer-living component, featuring instead transient absorption centred at about 580 nm, is ascribable to the fully relaxed LE state, which is thus the only minimum reached in the excited state deactivation of ***Pyr*** within the hydrogels. Hence, the position of the steady-state emission spectra recorded in these supramolecular assemblies (540 nm in *p*DoAO Gel and 535 nm in *Gemini* Gel) is in a higher energy region, where the fluorescence originated from the LE state is known to fall on ($\lambda_{max,LE}$ = 545 nm, cf. Table 2); differently from the emission coming from the TICT and PICT states which can be found at longer wavelength and very close in energy to one another ($\lambda_{max,TICT}$ and $\lambda_{max,PICT}$ = 585 nm, cf. Table 2). The tremendous viscosity of the hydrogels poses an obstacle to molecular motions, therefore blocking any possible rotation and the planar LE state becomes the only emitting state.

These results support what had previously been observed for other N-methylpyridinium derivatives in the same viscous media.[24] At the end of the day, the considerable expertise developed in the handling of analogous molecules within the same surfactant systems[24] combined with a profound knowledge of the excited state dynamics of ***Pyr*** in solution[25] enabled to derive a deceptively straightforward interpretation of these compelling albeit complex data.

Experimental

Materials. The structure of *trans*-2-(1-pyrenyl)-ethenyl-1-methylpyridinium iodide (***Pyr***) is depicted in Chart 1. It was synthesized as an iodide salt for other works[1,17,18,25] following a procedure which has already been described for analogous compounds.[13,26]

The spectroscopic investigation performed in micellar media was carried out on samples prepared in deionized water as solvent (ELGA grade) in the presence of two anionic surfactants: sodium dodecyl sulfate (SDS) and potassium *p*-(octyloxy)benzene sulfonate (*p*OoBSK) (Chart 2). Micelle containing solutions were prepared with a surfactant concentration of 3×10^{-2} M, knowing that the critical micellar concentrations are 8×10^{-3} and 1×10^{-3} M for SDS[37] and *p*OoBSK,[23] respectively. The SDS surfactant was purchased from Sigma-Aldrich and purified by twice crystallization from methanol-acetone mixture, while the *p*OoBSK surfactant was synthesized and purified in our laboratories according to a procedure which has previously been reported in another work by the same authors.[23]

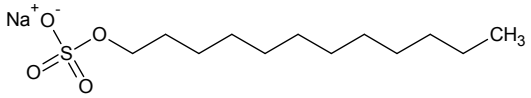

SDS

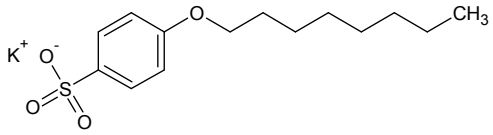

*p*OoBSK

Chart 2. Structures of the anionic surfactants used: sodium-dodecyl sulfate (SDS) and potassium *p*-(octyloxy)benzenesulfonate *(p*OoBSK*)*.

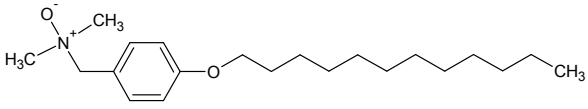

*p*DoAO

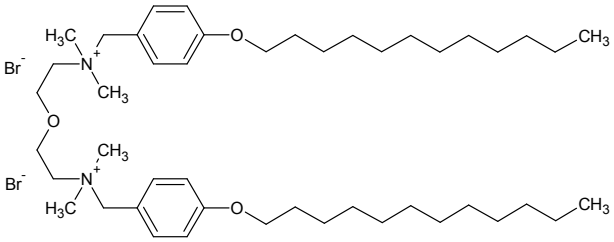

Gemini

Chart 3. Structures of *p*-dodecyloxybenzyldimethylamine N-oxide (*p*DoAO) and bis-[2-(N,N-dimethyl-N-p-dodecyloxybenzylammonium bromide)-ethyl]-ether (*Gemini*).

The zwitterionic and cationic surfactants (Chart 3), *p*-dodecyloxybenzyldimethylamine N-oxide (*p*DoAO) and bis-[2-(N,N-dimethyl-N-*p*-dodecyloxybenzylammonium bromide)-ethyl]-ether (*Gemini*), were also synthesized and purified in our laboratories and used at 0.067 M concentration to form homogeneous viscoelastic hydrogels for the confinement of the substrate, by means of experimental methods that have already been illustrated.[38-41]

The concentration of ***Pyr*** varied from a minimum of 3.0×10^{-6} M in the steady state measurements to a maximum of 2.0×10^{-4} M in the fluorescence up-conversion experiments, within a concentration range where aggregation is known not to occur.[1]

Methods. Steady-state absorption spectra were recorded with a Perkin Elmer Lambda 800 spectrophotometer, while a Fluorolog-2 (Spex, F112AI) spectrophotofluorometer was used to acquire steady-state emission spectra. The latter instrument gives back corrected fluorescence spectra taking into account the xenon lamp shape, the monochromator response and the detector sensitivity. 9,10-diphenilanthracene (ϕ_F = 0.73 in air-equilibrated cyclohexane)[42] was used as fluorimetric standard for the determination of the fluorescence quantum yield (ϕ_F) of the investigated compound in the micellar environment.

Fluorescein, whose ϕ_F has previously been found to be 1 in *p*DoAO hydrogel at pH 9,[38] was used as a standard to determine ϕ_F of the molecule in the viscoelastic solutions of both the *p*DoAO and *Gemini* surfactants.

The experimental setup for ultrafast spectroscopic and kinetic measurements has been widely used and described elsewhere.[43,44] The 400 nm excitation pulses of ca. 40 fs are generated by an amplified Ti:Sapphire laser system (Spectra Physics, Mountain View, CA). The transient absorption set up (Helios, Ultrafast Systems, Sarasota, FL) is characterized by a temporal resolution of ca. 150 fs and spectral resolution of 1.5 nm. Probe pulses for optical measurements are produced by passing a small portion of the 800 nm light through an optical delay line (with a time window of 3200 ps) and focusing it into a 2 mm thick sapphire window to generate a white-light continuum in the 475-800 nm range. The whole transient absorption spectrum is then collected at each delay step by a CCD detector. The chirp inside the sample cell is determined by measuring the laser-induced Kerr signal of water. In the up−conversion set−up (Halcyone, Ultrafast Systems, Sarasota, FL) the 400 nm pulses excite the sample whereas the remaining fundamental laser beam plays the role of the "optical gate" after passing through a delay line. The fluorescence of the sample is collected and focused onto a BBO crystal together with the delayed fundamental laser beam. The up-converted fluorescence beam is focused into the entrance of a monochromator using a lens, and it is then detected by a photomultiplier connected to a photon counter. Each experiment allows a single kinetic to be recorded. The time-resolved spectra are later reconstructed by calculating the fluorescence quantum flux function [Φ(t,λ)] at each wavelength. The temporal resolution of the up−conversion equipment is about 250 fs, whereas the spectral resolution is 5 nm. All of the ultrafast measurements were carried out under magic angle conditions, in a 2 mm cell and with an absorbance ranging from 0.3 to 1.0 at 400 nm. The samples were changed after every scan and kept in constant movement during the measurement by a magnetic stirrer for micellar solutions or, in the case of hydrogels, by a translational sample holder (Ultrafast Systems, Sarasota, FL) controlled by two NSC200 controllers (Newport, Irvine, CA), for horizontal and vertical displacement respectively, to prevent local photodegradation of the non-diffusing medium. However, no fluorescence up-conversion measurements were performed on hydrogel samples because of experimental difficulties, *i.e.* the need for a large number of equivalent samples to be investigated in order to collect information on a wide spectral window.

Transient absorption and fluorescence up-conversion data were analysed using the Surface Xplorer PRO (Ultrafast Systems, Sarasota, FL)[45,46] and Glotaran softwares.[47] The first allows to perform Global Analysis, giving lifetimes with an error of ~ 10% and Decay Associated Spectra, DAS, of the detected transients.[48] Glotaran was used to perform the Target Analysis, allowing the global fit of the acquired data to be carried out and providing the Species Associated Spectra (SAS).[47]

The fluorescence lifetimes (τ_F) were measured by a spectrofluorometer based on the single photon counting technique, equipped for the systems under investigation with a LED source centred at 461 nm using an interference filter centred at 460 nm in the excitation line and a long-pass filter in emission at 488 nm. The resolution time of the experimental set-up is about 200 ps when a LED source is used.[49] All the data acquired were analysed by IBH Data Analysis software; the program allows the decay profile of the source to be deconvoluted from the sample decay and provides the fitting of the data, whose goodness is evaluated by means of residuals distribution and the χ^2 value. The kinetic traces were also analysed by means of the Maximum Entropy Method (MEM) by means of the MEMEXP Software available online.[50,51] In the Maximum Entropy Method the experimental decay *I(t)* is fitted by the following function:

$$A(t) = D_0 \int_{-\infty}^{+\infty} d\log\tau[g(\log\tau) - h(\log\tau)] \times \int_{-t_0}^{\min(t,t_f)} dt' R(t') e^{-(t_i - t')/\tau} + \sum_{k=0}^{3} (b_k - c_k) \quad (1)$$

where *g(logτ)* and *h(logτ)* are the lifetime distributions that correspond to decay and rise kinetics, respectively, D_0 is a normalization constant, and the polynomial term accounts for the baseline. The instrument response function *R(t)* is peaked at zero time and is appreciable only in the interval $[-t_0, t_f]$. The fit procedure entails the maximization of the function Q defined in equation (2):

$$Q = S - \lambda C - \alpha I \quad (2)$$

In equation (2), *S* is entropy defined as:

$$S(\vec{f}, \vec{F}) = \sum_{j=1}^{M} [f_j - F_j - f_j \ln(f_j / F_j)] \quad (3)$$

where *f* is the image that includes both the *g* and the *h* lifetime distributions, whereas *F* is the MEM prior distribution used to incorporate prior knowledge into the solution. *C* is a measure of the quality of the fit *F* to the data. When we analysed the kinetic traces of femtosecond transient absorption with normally distributed noise, *C* was the χ^2. For Poisson-distributed data like those collected by the single photon counting technique, *C* was the Poisson deviance. *I* is a normalization factor; λ and α are Lagrange multipliers. The method, which is based on the simultaneous maximization of the entropy (*S*) and minimization of *C* (2), gives back the distribution of lifetimes, as well as the number of transients (family of distributions around an average time) needed to describe the spectroscopic kinetics. These distributions describe the probability of having different lifetimes. The widths of the distributions are sensitive to the heterogeneous microenvironment a molecule can experience in the sample.[52-55]

Conclusions

The investigated *push-pull* N-methylpyridinium compound, bearing a hydrophobic pyrene as donor substituent, is characterized by a low water-solubility, which limits its numerous potential applications especially in the medical field. Hence, the need for a strategy to better solubilize it and to understand its photophysics in response to changes in the experienced environment. Driven by the electrostatic attraction with anionic surfactants, the solubility of the molecule was promoted by inclusion within SDS and *p*OoBSK micellar aggregates, whereas its hydrophobicity fostered the permeation within gel matrixes.

Moreover, the excited state dynamics of the pyrenyl derivative shows peculiarities due to a specific interaction by π-stacking between the extended aromaticity of its pyrenyl substituent and the typical phenyl ring of those laboratory-synthesized surfactants conveniently chosen (*p*OoBSK, *p*DoAO and *Gemini*). Not only does this interaction greatly favor the inclusion of ***Pyr*** into the *p*OoBSK micellar aggregates and the hydrophobic domains of *p*DoAO and *Gemini* hydrogels, but it also severely limits the charge transfer processes and molecular rearrangements occurring during the excited state deactivation. The steady-state emission spectrum, which is generally scarcely affected by the diverse environments for N-methylpyridinium salts, results gradually blue-shifted when passing from non-surfactant solutions to surfactant micelles and surfactant hydrogels, because of a progressive hindrance to the rotation and thus to the fluorescence coming from the energetically stabilized TICT and PICT states, which are no longer populated in viscoelastic micellar solutions (cf. Scheme S1 summarizing the photo-induced processes occurring in the different media).

These features of ***Pyr***, together with its reasonable fluorescence quantum yield, makes it a good candidate for a potential application as fluorescent marker sensitive to changes in micro-viscosity. The inclusion in micelles and hydrogels allows the LE minimum to be labeled as the only emitting state in the viscous hydrogels. The change in colour of its emission, from yellow within the hydrogel to orange in aqueous medium, might therefore be useful for processing multi-valued logics.[55,56]

Acknowledgements

The authors acknowledge support from the Italian "Ministero per l'Università e la Ricerca Scientifica e Tecnologica", MIUR (Rome, Italy) under the FIRB "Futuro in Ricerca" 2013, no. RBFR13PSB6 and PRIN ''Programmi di Ricerca di Interesse Nazionale'' 2010–2011, no. 2010FM738P.

References

1 B. Carlotti, G. Consiglio, F. Elisei, C. G. Fortuna, U. Mazzucato and A. Spalletti, *J. Phys. Chem. A*, 2014, **118**, 3580.
2 P. Fromherz and A. Heilemann, *J. Phys. Chem.*, 1992, **96**, 6864.
3 H. Görner and H. Gruen, *J. Photochem.*, 1985, **28**, 329.
4 A. Battisti, S. Panettieri, G. Abbandonato, E. Jacchetti, F. Cardarelli, G. Signore, F. Beltram and R. Bizzarri, *Anal. Bioanal. Chem.*, 2013, **405**, 6223.
5 J. Bereiter-Hahn, K.-H. Seipel, M. Vöth and J. S. Ploem *Cell Biochem. Funct.*, 1983, **1**, 147.
6 P. Fromherz, K. H. Dambacher, H. Ephardt, A. Lambacher, C. O. Müller, R. Neigl, H. Schaden, O. Schenk and T. Vetter, *Ber. Bunsenges. Phys. Chem.*, 1991, **95**, 1333.
7 L. M. Loew, S. Scully, L. Simpson and A. S. Waggoner, *Nature*, 1979, **281**, 497.
8 V. Diemer, H. Chaumeil, A. Defoin, P. Jacques, C. Carré, *Tetrahedron Lett.*, 2005, **46**, 4737.
9 U. Narang, C.F. Zhao, J. D. Bhawalkar, F. V. Bright, P. N. Prasad, *J Phys. Chem.*, 1996, **100**, 4521.
10 C. F. Zhao, R. Gvishi, U. Narang, G. Ruland, P. N. Prasad, *J Phys. Chem.*, 1996, **100**, 4526.
11 C. G. Fortuna, C. Bonaccorso, F. Qamar, A. Anu and I. Ledoux, G. Musumarra, *Org. Biomol. Chem*., 2011, **9**, 1608.
12 G. He, G. Wang, R. Meng and Y. Cui, *Jpn. J. Appl. Phys.*, 2004, **43**, 1357.
13 C. G. Fortuna, G. Forte, V. Pittalà, A. Giuffrida and G. Consiglio, *Comput. Theor. Chem*., 2012, **985**, 8.
14 C. G. Fortuna, U. Mazzucato, G. Musumarra, D. Pannacci and A. Spalletti, *J. Photochem. Photobiol. A*, 2010, **216**, 66.
15 E. Marri, U. Mazzucato, C. G. Fortuna, G. Musumarra, A. Spalletti, *J. Photochem. Photobiol. A*, 2006, **79**, 314.
16 A. Mazzoli, A. Spalletti, B. Carlotti, C. Emiliani, C. G. Fortuna, L. Urbanelli, L. Tarpani, R. Germani, *J. of Phys. Chem. B,* 2015*,* **119**, 1483.
17 B. Carlotti, G. Consiglio, F. Elisei, C. G. Fortuna, U. Mazzucato and A. Spalletti*, J. Phys. Chem. A*, 2014, **118**, 7782.
18 A. Mazzoli, B. Carlotti, G. Consiglio, C. G. Fortuna, G. Miolo, and A. Spalletti, *Photochem. Photobiol. Sci.*, 2014,**13**, 939.
19 B Carlotti, A Cesaretti, C. G. Fortuna, A. Spalletti and F. Elisei, *Phys. Chem. Chem. Phys.*, 2015, **17**, 1877.
20 B. Carlotti, E. Benassi, A. Spalletti, C. G. Fortuna, F. Elisei and V. Barone, *Phys. Chem. Chem. Phys.*, 2014, **16**, 13984.
21 B. Carlotti, E. Benassi, V. Barone, G. Consiglio, F. Elisei, A. Mazzoli and A. Spalletti, *ChemPhysChem*, 2015, **16**, 1440.
22 E. Benassi, B. Carlotti, M. Segado, A. Cesaretti, A. Spalletti, F. Elisei and V. Barone, *J. Phys. Chem. B, 2015,* **119**, 6035.
23 A. Cesaretti, B. Carlotti, G. Consiglio, T. Del Giacco, A. Spalletti and F. Elisei, *J. Phys. Chem. B*, 2015, **119***,* 6658*.*
24 A. Cesaretti, B. Carlotti, R. Germani, A. Spalletti and F. Elisei, *Phys. Chem. Chem. Phys.*, 2015, **17**, 17214.
25 B. Carlotti, E. Benassi, A. Cesaretti, C. Fortuna, A. Spalletti, V. Barone and F. Elisei, *Phys. Chem. Chem. Phys.*, 2015, **17**, 20981.
26 C. G. Fortuna, V. Barresi, C. Bonaccorso, G. Consiglio, S. Failla, A. Trovato**–**Salinaro and G. Musumarra, *Eur. J. Med. Chem.,* 2012, **47**, 221.
27 V. P. Torchilin, *Pharm. Res.*, 2007, **24**, 1.
28 C. O. Rangel-Yagui, A. Pessoa Jr and L. C. Tavares, *J. Pharm. Pharm. Sci.*, 2005, **8**, 147.
29 C. Ghatak, V. G. Rao, S. Mandal, S. Ghosh and N. Sarkar, *J. Phys. Chem. B*, 2012, **116**, 3369.
30 A. Sanz-Medel, R. F. de la Campa and J. I. G. Alonso, *Analyst*, 1987, **112**, 493.
31 K. Bhattacharyya, *Acc. Chem. Res.*, 2003, **36**, 95.
32 S. K. Pal, D. Sukul, D. Mandal, S. Sen and K. Bhattacheryya, *Chem. Phys. Lett.*, 2000, **327**, 91.
33 N. Sarkar, A. Datta, S. Das and K. Bhattacharyya, *J. Phys. Chem.*, 1996, **100**, 15483.
34 K. Nishiyama, K. Takata, K. Watanabe and H. Shigematsu, *Chem. Phys. Lett.*, 2012, **529**, 39.
35 R. Baumann, C. Ferrante, E. Kneuper, F. W. Deeg and C. Brauchle, *J. Phys. Chem. A*, 2003, **107**, 2422.

36 S. K. Pal, D. Sukul, D. Mandal, S. Sen and K. Bhattacharyya, *J. Phys. Chem. B*, 2000, **104**, 2613.
37 B. L. Bales, L. Messina, A. Vidal and M. Peric, *J. Phys. Chem. B*, 1998, **102**, 1034.
38 A. Cesaretti, B. Carlotti, C. Clementi, R. Germani and F. Elisei, *Photochem. Photobiol. Sci.*, 2014, **13**, 509.
39 A. Cesaretti, B. Carlotti, P. L. Gentili, C. Clementi, R. Germani and F. Elisei, *Phys. Chem. Chem. Phys.*, 2014, **16**, 23096.
40 L. Brinchi, R. Germani, P. Di Profio, L. Marte, G. Savelli, R. Oda and D. Berti, *J. Colloid Interf. Sci.*, 2010, **346**, 100.
41 L. Goracci, R. Germani, G. Savelli and D. M. Bassani, *ChemBioChem*, 2005, **6**, 197.
42 G. Bartocci, F. Masetti, U. Mazzucato, A. Spalletti, I. Baraldi and F. Momicchioli, *J. Phys. Chem.*, 1987, **91**, 4733.
43 B. Carlotti, A. Cesaretti and F. Elisei, *Phys. Chem. Chem. Phys.*, 2012, **14**, 823.
44 A. Cesaretti, B. Carlotti, P. L. Gentili, C. Clementi, R. Germani and F. Elisei, *J. Phys. Chem. B*, 2014, **118**, 8601.
45 G. H. Golub and C. F. V. Loan, *Matrix Computations*, 1996.
46 G. Strang, Introduction to linear algebra, *Wellesley-Cambridge Press: Wellesley*, MA, 1998.
47 J. Snellenburg, S. Laptenok, R. Seger, K. Mullen and I. Van Stokkum, *J. Stat. Softw.*, 2012, **49**, 1.
48 I. H. van Stokkum, D. S. Larsen and R. van Grondelle, *Biochim. Biophys. Acta (Bioenergetics)*, 2004, **1657**, 82.
49 A. Romani, C. Clementi, C. Miliani, B. G. Brunetti, A. Sgamellotti and G. Favaro, *Appl. Spectrosc.*, 2008, **62**, 1395.
50 P. J. Steinbach, R. Ionescu and C. R. Matthews, *Biophys. J.*, 2002, **82**, 2244.
51 P. J. Steinbach, *J. Chem. Inf. Comput. Sci.*, 2002, 42, 1476.
52 M. Penconi, P. L. Gentili, G. Massaro, F. Elisei and F. Ortica, *Photochem. Photobiol. Sci.*, 2014, **13**, 48.
53 P. L. Gentili, C. Clementi and A. Romani, *Appl. Spectrosc.*, 2010, **64**, 923.
54 M. R. di Nunzio, P. L. Gentili, A. Romani and G. Favaro, *J. Phys. Chem. C*, 2010, **114**, 6123.
55 P. L. Gentili, *Dyes Pigments*, 2014, **110**, 235.
56 P. L. Gentili, *ChemPhysChem*, 2011, **12**, 739.

Table of Contents

The fluorescence of a N-methylpyridinium dye was modulated by nano-heterogeneous micellar systems, where its excited state twisting is gradually impaired by the increasing viscosity of the experienced medium.